

Solvent templated synthesis of metal-organic frameworks: structural characterisation and properties of the 3D network isomers
 $\{[\text{Mn}(\text{dcbp})] \cdot \frac{1}{2}\text{DMF}\}_n$ and $\{[\text{Mn}(\text{dcbp})] \cdot 2\text{H}_2\text{O}\}_n$

Eithne Tynan, Paul Jensen, Paul E. Kruger* and Anthea C. Lees
Department of Chemistry, Trinity College Dublin, Dublin 2, Ireland.
E-mail: Paul.Kruger@tcd.ie

Electronic Supplementary Information

Contents:

Synthesis of **1** and **2**

Figure ESI 1: Molecular structure and atomic numbering scheme for **2** and **2a** and schematic diagram showing the distortion of the dcbp ligand in **1**, **2** and **2a**.

Figure ESI 2: *bis*-Carboxylato chains found in **1** and **2**.

Figure ESI 3: Packing diagrams showing how the 3D networks in **1** and **2** differ.

Figure ESI 4: Packing diagrams of **1** showing the nature of the 3D network and additional views of its porous structure.

Figure ESI 5: Packing diagrams of **2** and **2a** showing the nature of the 3D network and additional views of their porous structures.

Figure ESI 6: TGA traces for **1** and **2**.

Synthesis of {[Mn(4,4'-dcbp)]·½ DMF}_n (1).

MnCl₂·4H₂O (56 mg, 0.285 mmol) and 4,4'-H₂dcbp (140 mg, 0.57 mmol) were placed in a 23ml Teflon[®]-lined digestion bomb with 2ml H₂O and 2ml DMF. The bomb was sealed, placed in an oven and heated to 200 °C for 16 hrs and then very slowly cooled to room temperature (3 °C/hr). Yellow plates, suitable for a single crystal diffraction study, were obtained directly in 80% yield.

The crystals are air stable and insoluble in water and common organic solvents.

IR (KBr): 1673(s), 1600(vs), 1558(s), 1427(m), 1397(s, sh), 1380(vs), 1289(w), 1256(w), 1233(w), 1141(w), 1089(w), 1011(w), 925(w), 905(w), 883(w), 786(m), 687(s), 571(w), 538(w), 501(w) cm⁻¹.

μ_B (300 K) = 5.80 B.M.

Found: C 48.24; H 2.64; N 10.29%. Required for Mn₂C₂₇H₁₉N₅O₉: C 48.59, H 2.87, N 10.49.

Synthesis of {[Mn(4,4'-dcbp)]·2H₂O}_n (2).

MnCl₂·4H₂O (56 mg, 0.285 mmol) and 4,4'-H₂dcbp (140 mg, 0.57 mmol) were placed in a 23ml Teflon[®]-lined digestion bomb with 4ml H₂O. The bomb was sealed, placed in an oven and heated to 200 °C for 16 hrs and then very slowly cooled to room temperature (3 °C/hr). Pale yellow needles were obtained in 74% yield.

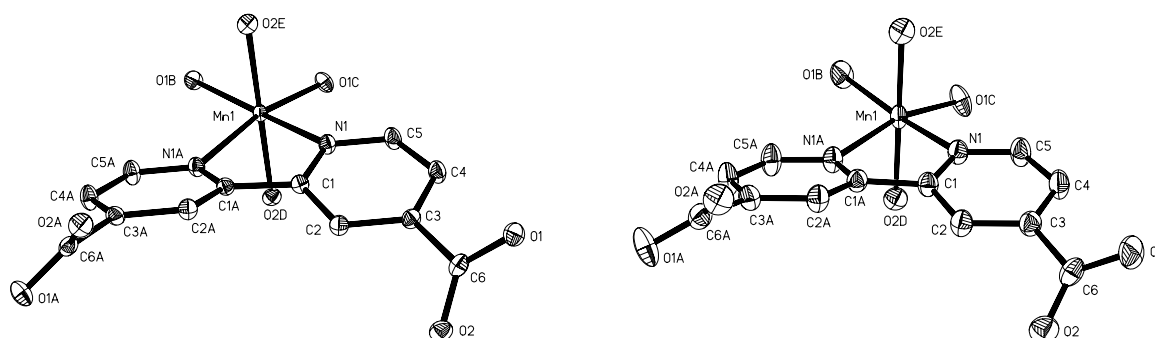
The yellow crystals are air stable and insoluble in common organic solvents.

IR (KBr): 3550(m, br), 3391 (w, br), 3230(w, br), 1600(vs), 1550(s), 1427(s, sh), 1408 (s, sh), 1383(vs), 1334(m, sh), 1296(w), 1228(w), 1151(w), 1113(w), 1010(w), 916(w), 863 (w), 791 (m), 690(vs), 597(w), 437(w) cm⁻¹.

Found: C 42.94, H 1.68, N 8.27%. Required for MnC₁₂H₁₀N₂O₆: C 43.26, H 3.03, N 8.41%.

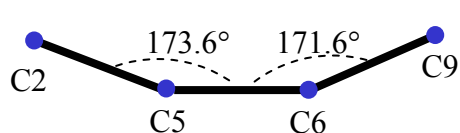
μ_B (300 K) = 5.70 B.M.

Figure ESI 1:

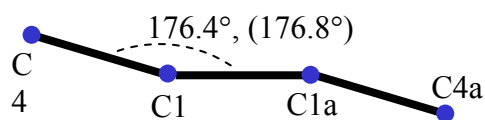


Molecular structure and atomic numbering scheme for **2** (left) and **2a** (right). Thermal ellipsoids are drawn to 50% probability level. Hydrogen atoms (and water for **2**) omitted for clarity. (**N.B.**, data were collected at 153 K for **2** and 343 K for **2a**.)

Note how the dcbp ligand is only slightly distorted across the central C1–C1a bond in **2** and **2a** [*i.e.* buckling across C4–C1–C1a, 176.4° (**2**) and 176.8° (**2a**)] compared with **1**, which is bent across C5–C6 *i.e.* C2–C5–C6 (173.6°) and C9–C6–C5 (171.6°). See below for a schematic illustration of this difference.

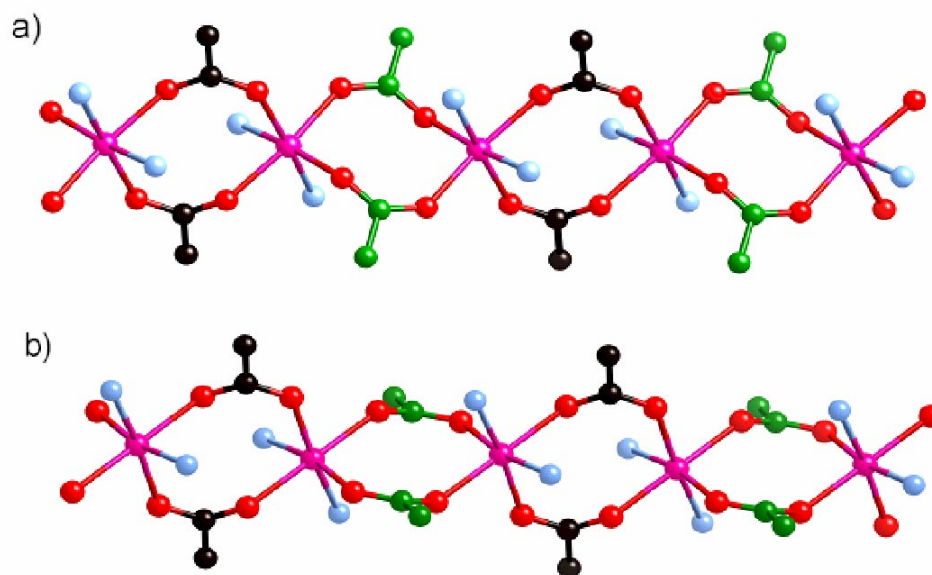


Bending of dcbp in **1**
across C5–C6



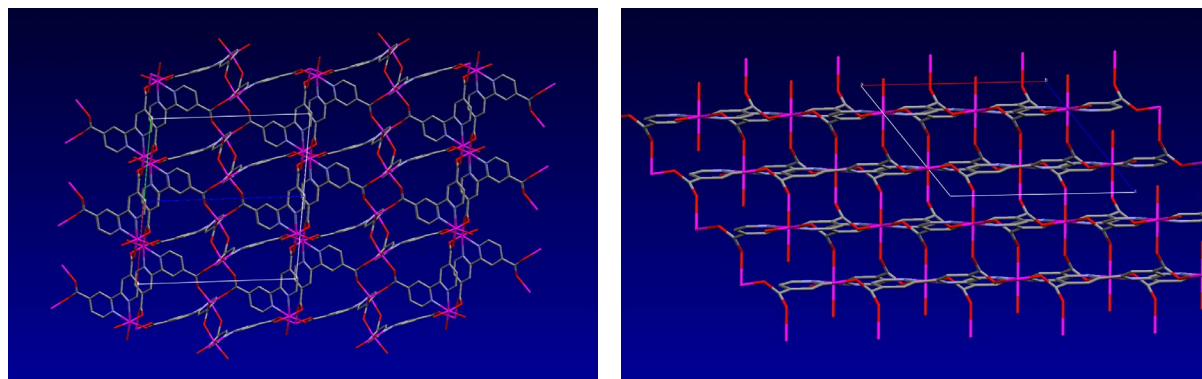
Buckling of dcbp in **2**
and (**2a**) across C1–C1a

Figure ESI 2:



bis-Carboxylato bridged manganese chains in (a) **1** and (b) **2**. The black carbons are oriented in the same direction in the two chains, whereas the green carbons in **1** are pointing in a different direction to those in **2**, thus resulting in a different orientation for the 4,4'-dcbp ligands and hence different linking of the chains in the two structures.

Figure ESI 3:



Packing diagrams of the networks in **1** (left, viewed down -110) and **2** (right, viewed down the b -axis) showing the relationship between the *bis*-carboxylato chains and demonstrating how the networks differ. Note how in **1** the chains run down (110) and (-110) and subtend an angle of *ca.* 66° to each other, whereas in **2** they run parallel with each other and along the c -axis. (see **ESI Fig 4** and **5** for further packing diagrams).

Figure ESI 4: Packing diagrams of **1** viewed down: a , c , and 110 , respectively.

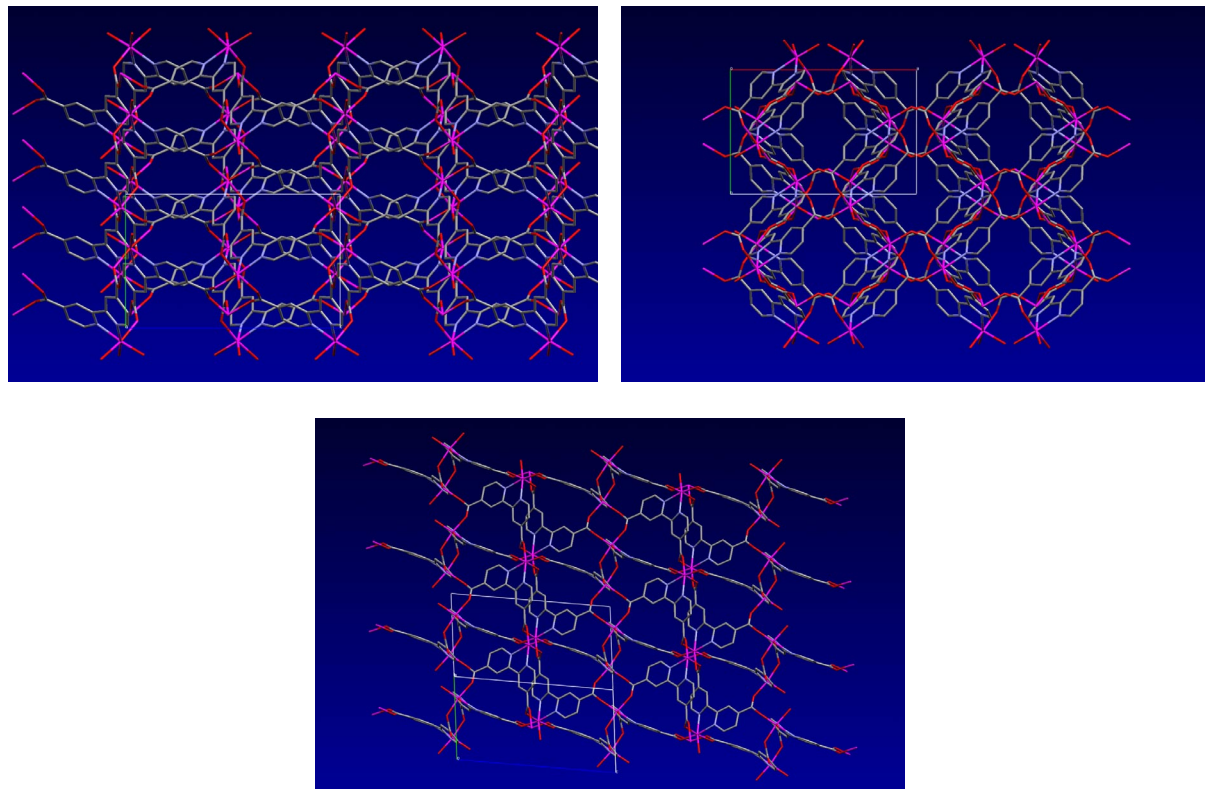


Figure ESI 5: Packing diagrams of **2** (top) and **2a** (bottom) viewed down: a , and 101, respectively. Note the change in the torsion angles between the pyridyl rings on going from **2** to **2a**.

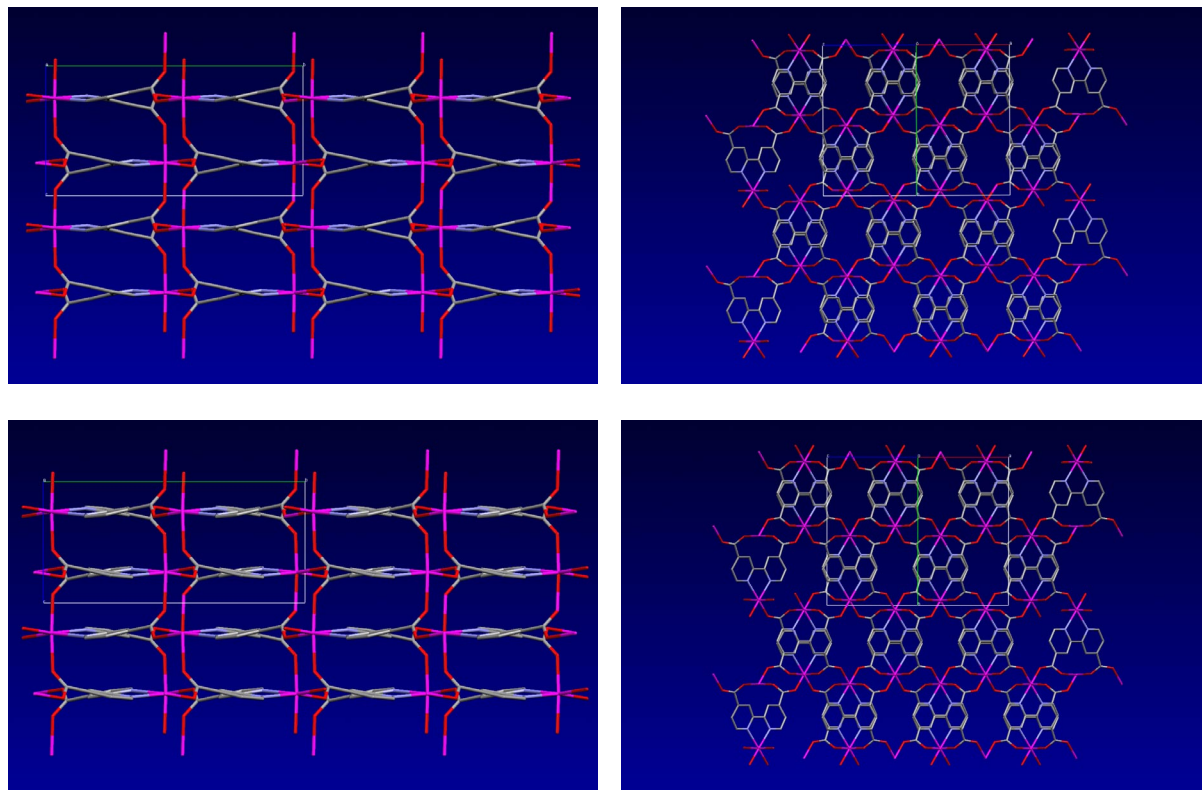


Figure ESI 6: TGA traces for **1** and **2** (heating rate *ca.* 10°C/min).

